Int. J. Heat Mass Transfer. Vol. 7, pp. 763–781. Pergamon Press 1964. Printed in Great Britain

HEAT TRANSFER IN ANNULAR PASSAGES. SIMULTANEOUS DEVELOPMENT OF VELOCITY AND TEMPERATURE FIELDS IN LAMINAR FLOW

H. S. HEATON,† W. C. REYNOLDS‡ and W. M. KAYS§

(*Received* 8 *November* 1963)

Abstract—An analysis is made of the problem of laminar flow heat transfer in an annulus with simultaneously developing velocity and temperature distributions and constant wall heat flux. A solution is obtained first for the hydrodynamic problem, and then for the combined hydrodynamic and thermal problem by an integral method. Results are tabulated for several inner to outer tube radius ratios and Prandtl numbers. Experimental measurements made for Prandtl number = 0·7 showed excellent agreement with the analysis. This paper is the fourth in a series culminating a four year study of heat transfer in annular passages.‖

NOMENCLATURE

A, area;
A_t, coefficient in temperature profile;
A_v, coefficient in velocity profile;
B, factor in fully developed velocity profile, $(r^{*2} - 1)/\ln r^*$;
B_t, coefficient in temperature profile;
B_v, coefficient in velocity profile;
bei ( ), Thomson function;
ber ( ), Thomson function;
C_t, coefficient in temperature profile;
C_v, coefficient in velocity profile;
c_1, constant used in equation (23);
c_p, specific heat at constant pressure;
D_h, hydraulic diameter, $2(r_o - r_i)$;
$\bar{D}_h$, normalized hydraulic diameter, D_h/r_o;
D_t, coefficient in temperature profile;
D_v, factor defined in equation (10);
E_t, coefficient in temperature profile;
F, factor defined where used;
$f_{1,2,3}$, functions of x used in several equations;
h, convective heat transfer coefficient;
I_n ( ), modified Bessel function of first kind of order n;
K_n ( ), modified Bessel function of second kind of order n;
k, thermal conductivity;
kei ( ), Thomson function;
ker ( ), Thomson function;
M, factor in fully developed velocity profile, $1 + r^{*2} - B$;
Nu, Nusselt number, hD_h/k;
Pr, Prandtl number, $c_p\mu/k$;
p, pressure;
q, heat rate;
q'', heat rate per unit area;
Re, Reynolds number, $u_m D_h/\nu$;
r, radial distance;
$\bar{r}$, normalized radial distance, r/r_o;
r^*, radius ratio, r_i/r_o;
$\bar{r}_m$, normalized distance to edge of thermal boundary layer;
t, temperature;
u, axial velocity;
$\bar{u}$, normalized velocity, u/u_m;
v, transverse velocity;
X, variable of integration defined in equation (16);
x, axial co-ordinate;
$\bar{x}$, normalized axial co-ordinate $(x/D_h)/(Re\ Pr)$;
Y, integrand defined in equation (16);
y, transverse co-ordinate;
Z, normalized axial co-ordinate, $(x/D_h)/Re$.

† Assistant Professor, Brigham Young University, Provo, Utah.
‡ Associate Professor, Stanford University, Stanford, California.
§ Professor, Stanford University, Stanford, California.
‖ The support of the National Aeronautics and Space Administration is gratefully acknowledged.

Greek symbols

α, thermal diffusivity, $k/\rho c_p$;
β, velocity profile parameter;
γ_o, βr_o;
γ_i, βr_i;
η_o, λr_o;
θ, dimensionless temperature, $(t - t_e)/(q_w'' D_h/k)$;
λ, temperature profile parameter;
μ, viscosity;
ν, kinematic viscosity, μ/ρ;
ρ, density;
ϕ, dimensionless temperature, $(t - t_w)/(q_w'' r_o/k)$, or $(t - t_w)/(q_w'' y_o/k)$.

Subscripts

c, location of maximum velocity;
e, entrance ($x = 0$);
fd, fully developed;
i, inner wall;
m, mixed-mean;
n, index (0, 1, 2, . . .);
o, outer wall;
w, wall (i or o);
ii, inner wall conditions, when inner wall alone is heated;
oo, outer wall conditions, when outer wall alone is heated;
io, inner wall conditions, when outer wall alone is heated;
oi, outer wall conditions, when inner wall alone is heated;
mi, mixed mean conditions, when inner wall alone is heated;
mo, mixed mean conditions, when outer wall alone is heated.

1. INTRODUCTION

THIS paper is part of a series [1–3] on an extensive study of convective heat transfer in an annular passage. All the papers of the series up to now have considered only fully developed flow in the heated portion of the annulus. This paper describes an analytical and experimental study of heat transfer in an annulus in which the velocity is uniform at the entrance and the heating begins at the entrance. Thus both the velocity and temperature distributions develop simultaneously.

When fluid enters a duct from a large chamber, a hydrodynamic boundary layer begins to develop on the wall of the duct. As the fluid progresses downstream, the boundary layer on one wall thickens until it begins to intercept the boundary layer from the opposite wall. At this point the boundary layers begin to loose their identity and a non-varying velocity distribution across the duct is approached. The thermal boundary layer develops in a similar fashion.

Normally the hydrodynamic boundary layer begins laminar and then undergoes transition to turbulent flow at some distance downstream depending on the Reynolds number, turbulence intensity, type of inlet and several other factors. If the turbulence intensity is low and the inlet is smooth, the laminar flow may persist far downstream, even for diameter Reynolds numbers much greater than the value of about 2100 commonly associated with transition in a tube. For example, in the present study, laminar flow in a circular tube was found to remain for 13 diameters at a Reynolds number of 27 000. For a certain annulus, laminar flow was found to remain for 11 times the hydraulic diameter with a Reynolds number of over 29 000 with transition occurring a little sooner on the inner wall than on the outer wall. It can be seen that an investigation of heat transfer near the entrance of a duct should include a consideration of laminar flow.

The present study is restricted to laminar incompressible flow. The assumption of incompressible flow along with the assumption that other properties are not temperature dependent allows an independent solution of the hydrodynamic problem, since the momentum and energy equations are not coupled.

With simultaneous development of both velocity and temperature fields, the Prandtl number becomes a more significant parameter because its effect can no longer be included entirely in the dimensionless axial variable. The Prandtl number represents the ratio of momentum diffusion to thermal diffusion and thus indicates the relative growth of the hydrodynamic boundary layer compared to the thermal boundary layer.

The boundary conditions considered for this problem are one wall heated and the other insulated. This corresponds to the fundamental

solution of the second kind according to the nomenclature introduced in [1]. By superposition this may be extended to constant but different heat flux on each wall.

The differential equations associated with this problem are the continuity equation, the momentum equation, and the energy equation as given below in cylindrical co-ordinates.

$$\frac{\partial u}{\partial x}+\frac{v}{r}+\frac{\partial v}{\partial r}=0 \tag{1}$$

$$u\frac{\partial u}{\partial x}+v\frac{\partial u}{\partial r}=-\frac{1}{\rho}\frac{\partial p}{\partial x}+\nu\left(\frac{\partial^2 u}{\partial r^2}+\frac{1}{r}\frac{\partial u}{\partial r}\right) \tag{2}$$

$$u\frac{\partial t}{\partial x}+v\frac{\partial t}{\partial r}=\alpha\left(\frac{\partial^2 t}{\partial r^2}+\frac{1}{r}\frac{\partial t}{\partial r}\right) \tag{3}$$

The co-ordinate system is shown in Fig. 1.

These equations assume steady, laminar, incompressible flow with constant fluid properties and negligible axial conduction, internal energy generation, viscous energy dissipation, and axial rate of change of radial shear stress.

Because the momentum equation (2) is non-linear in u, it is difficult to solve by exact methods. Instead, an approximate solution was obtained for both the hydrodynamic problem and the combined hydrodynamic and thermal problem by an integral method. The results are obtained for $r^* = 0$, 0·02, 0·05, 0·1, 0·25, 0·5, 1·0 and $Pr = 0{\cdot}01$, 0·7, 10·0.

In addition to the theoretical work, an experimental heat-transfer study was conducted using air ($Pr = 0{\cdot}7$) as a fluid for $r^* = 0{\cdot}029$, 0·058, 0·191, 0·255, 0·375, 0·500.

2. HYDRODYNAMIC ENTRY LENGTH PROBLEM

As yet, no exact solutions have yet been obtained for developing flow in an annulus. Murakawa [4] has obtained an approximate entrance length solution for the annulus by a series solution. The final result only partially satisfies the boundary conditions.

A number of approximate solutions have been obtained for the circular tube and parallel plates. A particularly simple solution for the circular tube by the integral method was obtained by Schiller [5] who assumed a parabolically varying velocity in the boundary layer and a potential flow core. The flow became fully developed abruptly when the boundary layers met at the center. Sparrow [6] did a similar solution for the parallel plates. Several later modifications have been made to the Schiller solution.

Another important integral method solution was found by Langhaar [7] for the circular tube, and later by Han [8] for the parallel plates. Langhaar obtained a velocity profile defined over the entire channel by linearizing the momentum equation.

The method of Langhaar applied to the annulus will be used here because of the simplicity of a single expression for velocity over the entire flow fleld for later use in the heat-transfer solution. This method gives a velocity profile which asymptotically approaches the exact fully developed profile, and for the circular tube and parallel plates gives reasonably accurate results when compared to finite difference solutions or experimental data.

The first step in obtaining the solution is to determine a velocity profile expression for use in the momentum integral equation. Far downstream from the entrance the momentum equation (2) becomes,

$$\frac{\partial^2 u}{\partial r^2}+\frac{1}{r}\frac{\partial u}{\partial r}=\frac{1}{\mu}\frac{\partial p}{\partial x}=\text{Const.} \tag{4}$$

The solution of this equation and boundary conditions gives Lamb's fully developed velocity

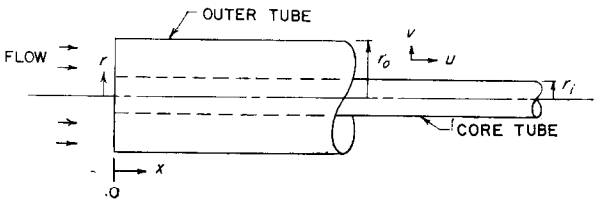

FIG. 1. Co-ordinate system.

profile for the annulus expressed below in dimensionless variables as,

$$\bar{u} = \frac{2}{M}(1 - \bar{r}^2 + B \ln \bar{r}) \tag{5}$$

where $B = (r^{*2} - 1)/\ln r^*$ $M = 1 + r^{*2} - B$.

The left-hand side of (2) is non-zero in the entrance region, and because it is non-linear in u, serious difficulties arise in obtaining an exact solution. To allow an approximate solution in determining the developing velocity, it is assumed that the left-hand side of (2) is a linear function of u in the form $u\,\partial u/\partial x + v\,\partial u/\partial r = \beta^2 u$. The parameter β is assumed to be a function of x only and will remain unknown for now. This linearizing assumption can be interpreted as assuming the $v\,\partial u/\partial r$ term is relatively small and the velocity gradient $\partial u/\partial x$ is a function of x only. Over most of the flow field, $\partial u/\partial x$ and $\partial u/\partial r$ will be roughly the same order of magnitude and v will be small compared to u so that the assumption is reasonable. The region where the assumption is least accurate is very near the entrance and close to the wall. Note, however, that this assumption is made only to obtain a distribution of velocity and that this assumption is not made in the momentum integral equation which gives the final solution.

With this simplification, (2) may be written as

$$\frac{\partial^2 u}{\partial r^2} + \frac{1}{r}\frac{\partial u}{\partial r} - \beta^2 u = f_1(x) \tag{6}$$

The function $f_1(x)$, which represents the pressure gradient, can also be expressed as a function of β.

The boundary conditions for (6) are

$$\begin{aligned} &u(r_i,x) = 0 \quad \text{(a)} && v(r_i,x) = 0 \quad \text{(d)} \\ &u(r_o,x) = 0 \quad \text{(b)} && v(r_o,x) = 0 \quad \text{(e)} \\ &u(r,0) = u_m \quad \text{(c)} \end{aligned} \tag{7}$$

Equation (6) can be represented as a form of Bessel's equation and the solution in terms of $\gamma_o = \beta r_o$ and other dimensionless variables may be written as,

$$\bar{u} = A_v I_o(\gamma_o \bar{r}) + B_v K_o(\gamma_o \bar{r}) + C_v \tag{8}$$

The coefficients A_v, B_v, C_v are functions of γ_o and r^* only.

The continuity integral equation

$$\int_{r^*}^{1} \bar{u}\,\bar{r}\,d\bar{r} = (1 - \bar{r}^{*2})/2 \tag{9}$$

may be found from equations (1), (7c), (7d) and (7e). Using (9) and boundary conditions (7a) and (7b), the coefficients were found to be

$$\left.\begin{aligned} A_v &= 1/D_v \\ B_v &= -\left[\frac{I_o(\gamma_o) - I_o(\gamma_i)}{K_o(\gamma_o) - K_o(\gamma_i)}\right]\left(\frac{1}{D_v}\right) \\ C_v &= -B_v \cdot K_o(\gamma_o) - I_o(\gamma_o)/D_v \end{aligned}\right\} \tag{10}$$

where

$$\begin{aligned} D_v = {} & \frac{\gamma_o I_1(\gamma_o) - \gamma_i I_1(\gamma_i)}{(\gamma_o^2 - \gamma_i^2)/2} - I_o(\gamma_o) \\ & + \left[\frac{I_o(\gamma_o) - I_o(\gamma_i)}{K_o(\gamma_o) - K_o(\gamma_i)}\right]\left[\frac{\gamma_o K_1(\gamma_o) - \gamma_i K_1(\gamma_i)}{(\gamma_o^2 - \gamma_i^2)/2} + K_o(\gamma_o)\right] \end{aligned}$$

It can be shown by using asymptotic expansions for I_o and K_o, that for $\gamma_o \sim \infty$ and $x \sim 0$; equation (8) becomes $\bar{u} \sim 1$. Using series expansions for I_o and K_o it can be shown that for $\gamma_o \sim 0$ and $x \sim \infty$; equation (8) reduces to (5). Thus the velocity profile (8) approaches the limits exactly at the entrance and far downstream, and should provide an adequate approximation in the developing region.

The problem that now remains is to find the unknown β or γ_o as a function of axial distance by means of the momentum integral equation. To obtain the momentum integral equation, first (2) is multiplied by $r\,dr$ and then the result is integrated across the flow cross section.

$$\int_{r_i}^{r_o} u\frac{\partial u}{\partial x} r\,dr + \int_{r_i}^{r_o} v\frac{\partial u}{\partial r}\,r\,dr = -\frac{1}{\rho}\int_{r_i}^{r_o}\frac{\partial p}{\partial x}\,r\,dr + \nu\int_{r_i}^{r_o}\left(\frac{\partial^2 u}{\partial r^2} + \frac{1}{r}\frac{\partial u}{\partial r}\right) r\,dr \tag{11}$$

By means of the continuity equation (1) and boundary conditions (7) the two terms on the left of (11) can be shown to be identical. It is assumed that p is a function of x only so that the

first term on the right-hand side can be integrated directly with $\partial p/\partial x$ constant in the integration. At a certain radial location denoted by subscript c, the axial velocity will reach a maximum and therefore $(\partial u/\partial r)_c$ will be zero. Equation (2) at this point reduces to

$$\left(u\frac{\partial u}{\partial x}\right)_c = -\frac{1}{\rho}\left(\frac{\partial p}{\partial x}\right)_c + \nu\left(\frac{\partial^2 u}{\partial r^2}+\frac{1}{r}\frac{\partial u}{\partial r}\right)_c \quad (12)$$

Since p is independent of radial location, then

$$\frac{\mathrm{d}p}{\mathrm{d}x} = \left(\frac{\partial p}{\partial x}\right)_c$$

and the pressure gradient can be found from

$$-\frac{1}{\rho}\frac{\partial p}{\partial x} = \frac{\partial}{\partial x}\left(\frac{u_c^2}{2}\right) - \nu\left(\frac{\partial^2 u}{\partial r^2}+\frac{1}{r}\frac{\partial u}{\partial r}\right)_c \quad (13)$$

Note that determining the pressure in this manner allows for viscous effects in the core and does not assume a potential flow as in the Schiller [5] method.

By substituting (13), and combining the two right-hand terms and substituting dimensionless variables, (11) becomes

$$\frac{1}{\bar{D}_h^2}\frac{\mathrm{d}}{\mathrm{d}\bar{Z}}\left[\int_{r^*}^{1}\bar{u}^2\,\bar{r}\,\mathrm{d}\bar{r} - \bar{u}_c^2\left(\frac{1-r^{*2}}{4}\right)\right] = \int_{r^*}^{1}\left(\bar{r}\frac{\partial^2\bar{u}}{\partial\bar{r}^2}+\frac{\partial\bar{u}}{\partial\bar{r}}\right)\mathrm{d}\bar{r} - \left(\frac{\partial^2\bar{u}}{\partial\bar{r}^2}+\frac{1}{\bar{r}}\frac{\partial\bar{u}}{\partial\bar{r}}\right)_c\left(\frac{1-r^{*2}}{2}\right) \quad (14)$$

The axial co-ordinate is now

$$Z = \frac{x\nu}{D_h^2\,U_m} = \frac{x/D_h}{R_e}.$$

Equation (14) is the desired momentum integral equation.

Substituting the velocity profile (8) into (14) and evaluating the integrals, results in

$$\frac{\mathrm{d}X}{\mathrm{d}Z} = \frac{1}{Y} \quad (15)$$

where

$$X = C_v^2(1-r^{*2}) - (F_o^2 - r^{*2}F_i^2)/2 + \frac{2C_v}{\gamma_o}(F_o - r^{*2}F_i) - (F_c + C_v)\left(\frac{1-r^{*2}}{4}\right)$$

$$Y = \frac{1}{4\left[\gamma_o(F_o - r^*F_i) - \gamma_o^2\,\bar{r}_c\,F_c\left(\frac{1-r^{*2}}{2}\right)\right](1-r^*)^2} \quad (16)$$

$$F_o = A_v I_1(\gamma_o) - B_v K_1(\gamma_o)$$
$$F_i = A_v I_1(\gamma_i) - B_v K_1(\gamma_i)$$
$$F_c = A_v I_o(\gamma_o\bar{r}_c) + B_v K_o(\gamma_o\bar{r}_c)$$

The radius $\bar{r}_c$ at which $\partial\bar{u}/\partial\bar{r} = 0$ is determined from the expression,

$$A_v I_1(\gamma_o\bar{r}_c) - B_v K_1(\gamma_o\bar{r}_c) = 0 \quad (17)$$

Equation (15) can be integrated to give

$$Z = \int_{X(Z=0)}^{X(Z)} Y\,\mathrm{d}X \quad (18)$$

Because it was not feasible to solve (18) in closed form, a numerical solution was made. To do this it was necessary to find the values of X and Y at $Z = 0$. Using asymptotic expansions for the Bessel functions I_n and K_n, equations (16) were found to reduce to

$$\left.\begin{array}{l} X \sim (1-r^{*2})/4 \\ Y \sim 0 \end{array}\right\} \text{For } \gamma \to \infty,\ Z \to 0 \quad (19)$$

It was impractical to try to find a solution of the form $\gamma_o = \gamma_o(Z)$, so instead a solution of the form $Z = Z(\gamma_o)$ was found. The solution was carried out in the following way. For a series of values of γ_o starting with as large a value as possible and decreasing in steps close enough together to maintain the required accuracy in numerical integration, values of A_v, B_v and C_v were calculated from (10), and by trial and error, values of $\bar{r}_c$ were calculated from (17). After calculating X and Y from (16), Z was found from (18) by numerical integration. The results of the calculation are shown in Table 1. More detailed results are given in [9].

Some velocity profiles are shown in Fig. 2. It can be seen clearly from Fig. 2 the increasing asymmetry in the profile as the inner radius becomes small. In the figure for $r^* = 0{\cdot}001$, the fully developed profile for the circular tube is shown for comparison. Near the center, the very small core tube has a big effect on the velocity profile because of the zero velocity boundary

Table 1. Results of the hydrodynamic entry length solution for the annulus

	$r^* = 0.50$			$r^* = 0.25$			$r^* = 010$		
γ_0	z	$\bar{r}_c$	$\bar{u}_c$	z	$\bar{r}_c$	$\bar{u}_c$	z	$\bar{r}_c$	$\bar{u}_c$
50	$0.0_3 1267$	0.7468	1.0869	$0.0_4 5234$	0.6184	1.0563	$0.0_4 3539$	0.5390	1.0465
20	0.001020	0.7431	1.2333	$0.0_3 4171$	0.6099	1.1525	$0.0_3 2729$	0.5245	1.1245
10	0.003371	0.7393	1.3849	0.001798	0.5994	1.3015	0.001277	0.5052	1.2592
6.0	0.006088	0.7373	1.4545	0.003997	0.5914	1.4104	0.003209	0.4885	1.3842
4.0	0.008590	0.7364	1.4825	0.006405	0.5868	1.4673	0.005652	0.4777	1.4638
3.0	0.01046	0.7360	1.4932	0.008362	0.5847	1.4919	0.007813	0.4724	1.5028
2.0	0.01318	0.7358	1.5012	0.01134	0.5830	1.5116	0.01129	0.4679	1.5361
1.5	0.01530	0.7357	1.5040	0.01354	0.5824	1.5189	0.01396	0.4661	1.5492
1.0	0.01968	0.7356	1.5061	0.01679	0.5819	1.5243	0.01792	0.4648	1.5591
0	∞	0.7355	1.5078	∞	0.5815	1.5287	∞	0.4637	1.5673
	$r^* = 0.05$			$r^* = 0.02$			$r^* = 0.001$		
γ_0	z	$\bar{r}_c$	$\bar{u}_c$	z	$\bar{r}_c$	$\bar{u}_c$	z	$\bar{r}_c$	$\bar{u}_c$
50	$0.0_4 3151$	0.5108	1.0439	$0.0_4 2945$	0.4917	1.0425	$0.0_4 2810$	0.4717	1.0415
20	$0.0_3 2400$	0.4919	1.1170	$0.0_3 2221$	0.4677	1.1128	$0.0_3 2092$	0.4357	1.1095
10	0.001144	0.4665	1.2465	0.001070	0.4352	1.2389	0.001021	0.3868	1.2328
6.0	0.003015	0.4438	1.3771	0.002932	0.4055	1.3744	0.002978	0.3413	1.3780
4.0	0.005551	0.4286	1.4680	0.005624	0.3852	1.4764	0.006135	0.3101	1.5015
3.0	0.007903	0.4209	1.5152	0.008232	0.3748	1.5323	0.009424	0.2945	1.5754
2.0	0.01181	0.4143	1.5573	0.01271	0.3659	1.5841	0.01535	0.2812	1.6479
1.5	0.01487	0.4116	1.5743	0.01627	0.3623	1.6055	0.02021	0.2761	1.6790
1.0	0.01944	0.4097	1.5873	0.02163	0.3597	1.6220	0.02762	0.2722	1.7036
0	∞	0.4080	1.5982	∞	0.3574	1.6361	∞	0.2690	1.7248

condition on the wall, while near the outer wall the profiles are nearly identical.

In Fig. 3 is shown maximum velocity as a function of the axial distance parameter for various radius ratios. Also shown as a dotted line is the fully developed condition defined by $\bar{u}_c/(\bar{u}_c)_{fd} = 0.99$.

3. THERMAL ENTRY LENGTH PROBLEM

The common method of solving the thermal entry length problem in ducts with fully developed flow is by the method of separation of variables. This method is not applicable to the case of developing flow because here the velocity is a non-separable function of the two co-ordinate variables.

Several approximate solutions have been obtained for the parallel plates and circular tube. A finite difference solution has been obtained by Kays [10] and Goldberg [11] for the circular tube. Shibahayasi and Sugino [12] have obtained a solution for the circular tube assuming the boundary layer is thin. Sparrow [6], and Siegel and Sparrow [13], have obtained solutions for the parallel plates by an integral method using a temperature profile similar to that used by Schiller [5] for the hydrodynamic boundary layer. Han [14] has also solved the parallel plate problem by an integral method, but he found a temperature profile in a way similar to that used by Langhaar [7] to find the developing velocity profile.

Murakawa [4] has obtained a solution for arbitrary wall temperature at the inner wall of the annulus by an integral method. The developing velocity and temperature profiles used were quite simplified and only applicable near the inner wall. The resulting solution did not show all the effects of radius ratio nor did it approach the fully developed solution.

The solution obtained here is by an integral method using a temperature profile found by the same general technique used to find the velocity profile. The method is in many respects similar to that used by Han [14] for the parallel plates.

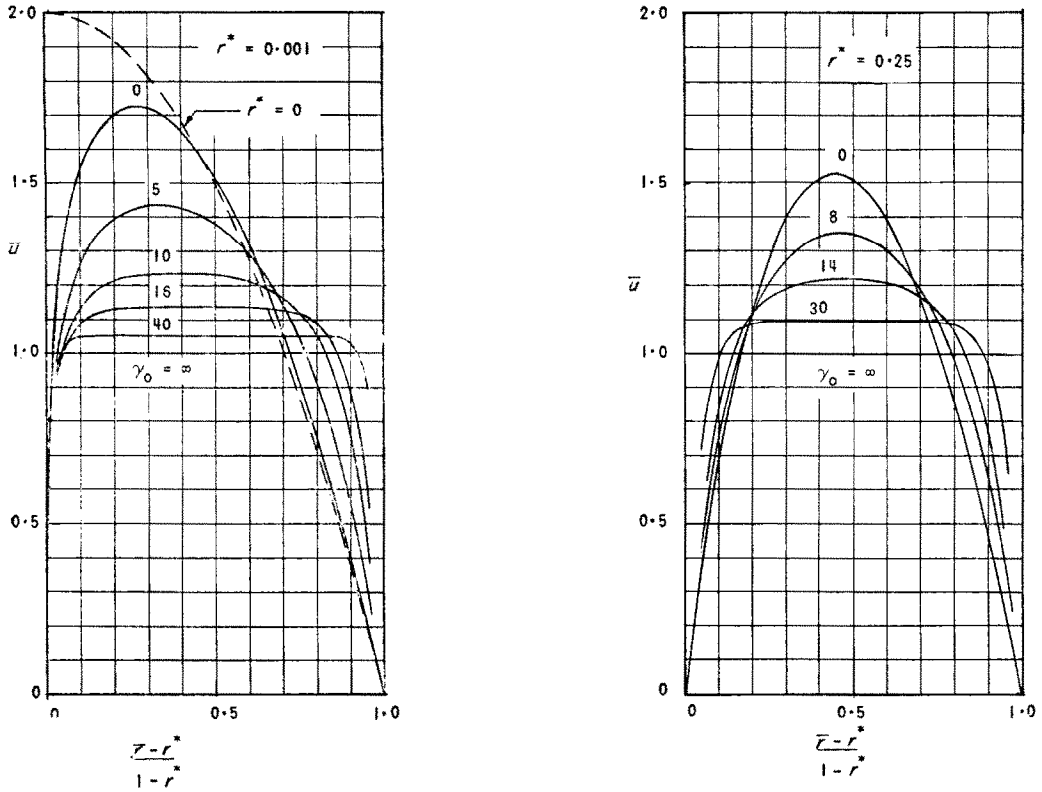

FIG. 2. Developing velocity profiles for the annulus.

To find the temperature profile in the developing region, equations (1), (2) and (3) will be solved approximately in terms of an unknown parameter which can be determined from the energy integral equation. The boundary conditions first considered are for the inner wall heated with a constant heat flux and the outer wall insulated. These can be expressed for $t(x, r)$ as,

$$\left.\begin{aligned} & t(0, r) = t_e \\ & \frac{\partial t}{\partial r}(x, r_i) = -q_i''/k \\ & \frac{\partial t}{\partial r}(x, r_o) = 0 \\ & t(\infty, r) = t_{fd} \end{aligned}\right\} \quad (20)$$

Far downstream from the entrance where both temperature and velocity are fully developed, equations (2) and (3) can be combined to give,

$$\nabla^2\nabla^2 t = \frac{1}{\alpha}\frac{1}{\mu}\frac{\partial t}{\partial x}\frac{\partial p}{\partial x} = \text{Const.} \quad (21)$$

where

$$\nabla^2 = \frac{\partial^2}{\partial r^2} + \frac{1}{r}\frac{\partial}{\partial r}$$

Defining a new temperature variable

$$\phi = \frac{t - t_i}{q_i'' r_o/k} \quad (22)$$

and substituting into (21) gives

$$\nabla^2\nabla^2\phi = c_1 = \text{Const.} \quad (23)$$

The solution to this equation and boundary conditions is

$$\phi_{fd} = \frac{\bar{D}_h r^*}{M(1 + r^*)(1 - r^*)^2}\left[\frac{(1 - B)}{2}(\bar{r}^2 - \ln \bar{r}) - \frac{\bar{r}^4}{8} + \frac{B}{2}\bar{r}^2 \ln \bar{r} - \frac{\bar{r}^{*2} M}{2} + \frac{1 + \ln r^*}{2} + \frac{r^{*4}}{8}\right] \quad (24)$$

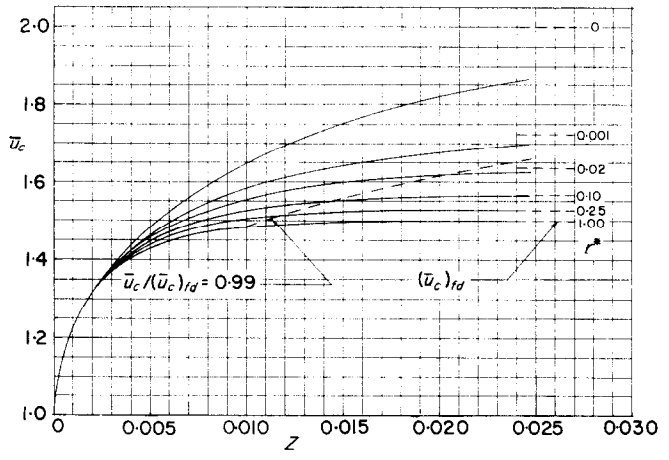

FIG. 3. Maximum velocity variation in the entry region of an annulus.

For developing conditions when equations (2) and (3) are similarly combined, there are several more terms which make it virtually impossible to obtain a direct solution for a temperature profile. To simplify the resulting equation in a manner similar to that used for determining the velocity profile, the additional terms are approximated by a linear function ϕ and c_1 becomes a function of x that will be called $f_2(x)$. The approximate equation becomes,

$$\nabla^2\nabla^2\phi = f_2(x) - \lambda^4\phi \tag{25}$$

The parameter λ is assumed to be a function of x only and will remain as an unknown for now.

The physical interpretation and justification of this approximation is not as clear as it is for the velocity problem. However, the purpose here is to obtain a reasonably accurate variation of temperature in the developing region to be used in the energy integral equation, which satisfies the boundary conditions, initial conditions, and fully developed conditions. The resulting temperature does satisfy the necessary conditions and does appear to give an excellent approximation to the developing region except for a slight irregularity which is accounted for later. An earlier attempt was made to find a temperature distribution using a polynomial, but it was found that for small radius ratios, so many terms in the polynomial were required to give a reasonable result that it was impractical.

Checking the profile at the limits, for $\lambda = 0$, (25) becomes identical to (23) so that $\phi = \phi_{fd}$. For $\lambda \to \infty$, it can be shown that ϕ approaches zero so that this represents the profile at the entrance. Thus for $x \sim 0$; $\lambda \sim \infty$, and for $x \sim \infty$; $\lambda \sim 0$. The parameter λ for the temperature profile has a similar behavior as β for the velocity profile.

Substituting dimensionless variables and $\eta_o = \lambda r_o$ into (25), (20) and (3) gives the differential equation and boundary conditions necessary to find the temperature profile.

$$\left(\frac{\mathrm{d}^2}{\mathrm{d}\bar{r}^2} + \frac{1}{\bar{r}}\frac{\mathrm{d}}{\mathrm{d}\bar{r}}\right)\left(\frac{\mathrm{d}^2\phi}{\mathrm{d}\bar{r}^2} + \frac{1}{\bar{r}}\frac{\mathrm{d}\phi}{\mathrm{d}\bar{r}}\right) + \eta_o^4\phi = f_3(x) \tag{26}$$

$$\left.\begin{aligned} &\left.\begin{aligned} &\phi = 0 \\ &\frac{\partial\phi}{\partial\bar{r}} = -1 \\ &\frac{\partial^2\phi}{\partial\bar{r}^2} + \frac{1}{\bar{r}}\frac{\partial\phi}{\partial\bar{r}} = 0 \end{aligned}\right\} \text{at } \bar{r} = r^* \\ &\left.\begin{aligned} &\frac{\partial\phi}{\partial\bar{r}} = 0 \\ &\frac{\partial^2\phi}{\partial\bar{r}^2} + \frac{1}{\bar{r}}\frac{\partial\phi}{\partial\bar{r}} = 0 \end{aligned}\right\} \text{at } \bar{r} = 1 \end{aligned}\right\} \tag{27}$$

The function $f_3(x)$ can be represented as a function of η_o.

The homogeneous part of equation (26) is a form of Bessel's equation with solutions $I_o(\eta_o \bar{r}\sqrt{i})$

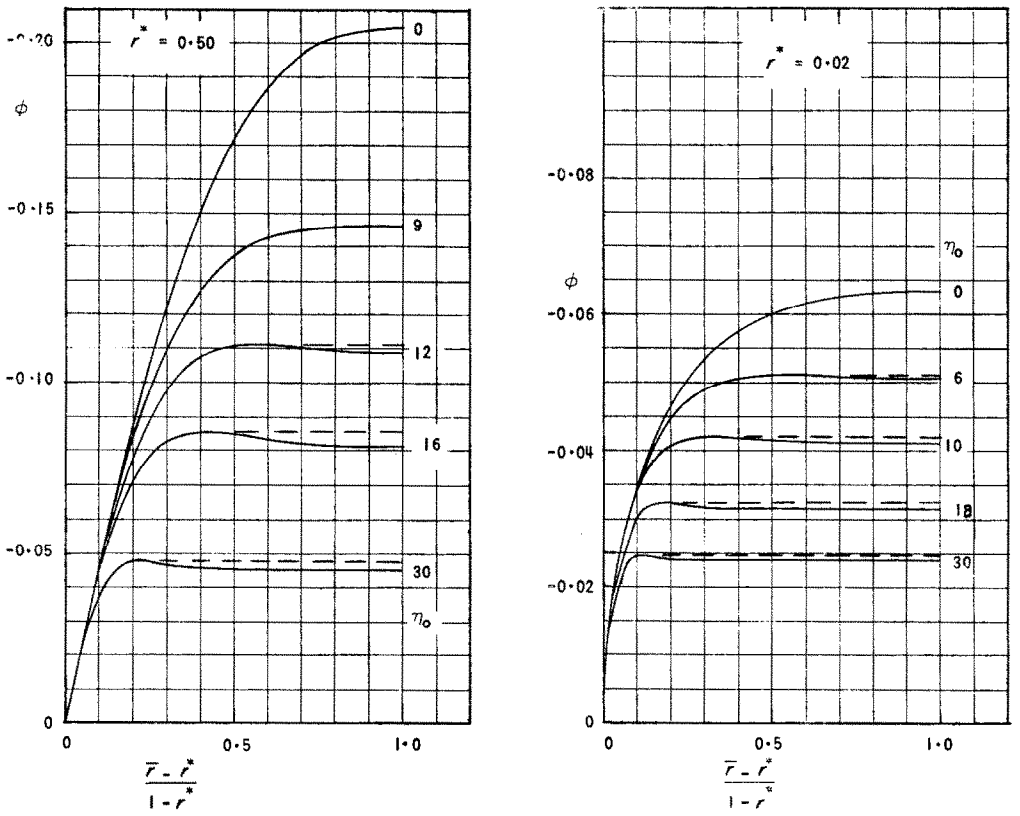

FIG. 4. Developing temperature profiles for the annulus with the inner wall heated.

and $K_0(\eta_0 \bar{r}\sqrt{i})$. These solutions are commonly written in terms of the Thomson functions: ber, bei, ker, kei. The solution to (26) then becomes

$$\phi = A_t \text{ ber}(\eta_0\bar{r}) + B_t \text{ bei}(\eta_0\bar{r}) + C_t \text{ ker}(\eta_0\bar{r}) + D_t \text{ kei}(\eta_0\bar{r}) + E_t \quad (28)$$

The coefficients A_t, B_t, C_t, D_t, E_t are functions of η_0 and r^* and may be determined from the boundary conditions (27). The equations for the coefficients are rather lengthy and will not be presented here. They are presented in detail in [9] along with calculated numerical values. Several temperature profiles calculated from equation (28) are shown graphically in Fig. 4.

It is noted from Fig. 4 that the profiles near the entrance are regular next to the inner wall, but in the middle of the stream and near the outer wall there is a slight dip in the profile. This dip is contrary to the physical situation and is the result of the approximation made in simplifying the differential equation. In later work only that part of the profile calculated from equation (28) from the inner wall to where $-\phi$ is maximum will be used. This is in effect considering only the part of the profile which represents the effective thermal boundary layer. Outside the boundary layer the fluid has not felt the heating from the wall and is still at the initial temperature. When the boundary layer reaches the opposite wall there is no difficulty with equation (28).

The energy integral equation may be found by integrating the energy differential equation (3) across the flow cross section and simplifying by means of the continuity equation (1) and boundary conditions. In terms of dimensionless variables, the energy integral equation may be written as,

$$\frac{\mathrm{d}}{\mathrm{d}\bar{x}}\int_{r^*}^{1} \bar{u}\left(\frac{t - t_e}{q_t'' r_0/k}\right)\bar{r}\,\mathrm{d}\bar{r} = r^*\bar{D}_h^2 \quad (29)$$

The axial distance parameter convenient for the thermal problem is

$$\bar{x} = \frac{x\alpha}{D_h^2 u_m} = \frac{x/D_h}{Re\,Pr} = \frac{Z}{Pr}$$

There are two regions in which (29) may be represented. First is the region in which the effective thermal boundary layer described earlier (the outside dimension is denoted by $\bar{r}_m$) has not yet reached the outer wall. It is assumed in this region that the fluid outside the boundary layer is at the inlet temperature. Equation (29) in this region may be integrated and written as

$$\bar{x} = \frac{1}{r^* \bar{D}_h^2}\left[\int_{r^*}^{\bar{r}_m} \phi\,\bar{u}\,\bar{r}\,\mathrm{d}\bar{r} - (\phi)_{\bar{r}=\bar{r}_m}\int_{r^*}^{\bar{r}_m} \bar{u}\,\bar{r}\,\mathrm{d}\bar{r}\right] \quad (30)$$

where

$$-(\phi)_{r=\bar{r}_m} = \frac{t_i - t_{\bar{r}=\bar{r}_m}}{q_i'' r_o/k} = \frac{t_i - t_e}{q_i'' r_o/k}$$

In the second region the effective thermal boundary layer has reached the outer wall and equation (28) applies across the entire cross section. Equation (29) in this region may be integrated and written as

$$\bar{x} = \frac{1}{r^* \bar{D}_h^2}\left[\int_{r^*}^{1} \phi\,\bar{u}\,\bar{r}\,\mathrm{d}\bar{r} + \left(\frac{t_i - t_e}{q_i'' r_o/k}\right)\left(\frac{1 - r^{*2}}{2}\right)\right] \quad (31)$$

In this region the outer wall has begun to increase in temperature so that $t_o \neq t_e$ and a different method must be used to get $t_i - t_e$ in terms of ϕ. At the point $r = r_c$; $(\partial u/\partial r) = 0$ and $v \approx 0$, and equation (2) becomes

$$u_c\left(\frac{\partial t}{\partial x}\right)_c = \alpha\left(\frac{\partial^2 t}{\partial r^2} + \frac{1}{r}\frac{\partial t}{\partial r}\right)_c \quad (32)$$

Integrating (32) with respect to x and substituting dimensionless variables gives

$$\frac{t_i - t_e}{q_i'' r_o/k} = \int_0^{\bar{x}} \frac{1}{\bar{u}_c}\left\{\frac{\partial^2\phi}{\partial\bar{r}^2} + \frac{1}{\bar{r}}\frac{\partial\phi}{\partial\bar{r}}\right\}_c \mathrm{d}\bar{x} - \phi_c \quad (33)$$

where

$$\phi_c = \frac{t_c - t_i}{q_i'' r_o/k}$$

Equations (31) and (33) give the necessary equations for the second region.

The integrals in (30) and (31) were found by substituting the velocity profile (8) and the temperature profile (28) and then evaluating the resulting 15 integrals. The final results of this are given in [9].

It is desired now to find $\bar{x} = \bar{x}(\eta_o)$ from equations (30) and (31) and the hydrodynamic solution which gives $Z = Z(\gamma_o)$. The relation between the axial co-ordinates Z and $\bar{x}$ is

$$\bar{x} = \frac{Z}{Pr} \quad (34)$$

The solution was found by a trial and error procedure. The general steps of this procedure are, for a given Pr and r^*:

(1) Choose a value of γ_o for which the hydrodynamic solution gives Z.
(2) Calculate $\bar{x}$ from equation (34).
(3) Assume a value of η_o and using equations (30) or (31), calculate $\bar{x}$.
(4) Repeat step (3) until the value of $\bar{x}$ agrees with that found in step (2).

The final results are η_o and $\bar{x}$ as a function of γ_o for given values of Pr and r^*. The tabulated values of these variables along with the temperature profile (28) then give the solution to the problem of the inner wall heated uniformly and the outer wall insulated.

The mixed-mean fluid temperature is defined by

$$t_m = \int_{r_i}^{r_o} t\,u\,r\,\mathrm{d}r \Big/ \int_{r_i}^{r_o} u\,r\,\mathrm{d}r \quad (35)$$

In terms of dimensionless variables, the mixed-mean fluid temperature may be written as

$$\phi_m = \frac{t_m - t_i}{q_i'' r_o/k} = \frac{\int_{r^*}^{1} \phi\,\bar{u}\,\bar{r}\,\mathrm{d}\bar{r}}{(1 - r^{*2})/2} \quad (36)$$

The solution obtained here is the fundamental solution of the second kind,

$$\theta^{(2)} = \frac{t - t_e}{q_w'' D_h/k},$$

according to the designation given in [1]. Since only the solution of the second kind is considered here, the superscript (2) will be dropped.

The convenient representations of this fundamental solution consistent with those given in [2] for fully developed velocity throughout are given below in terms of the nomenclature used here.

$$\theta_{ii} - \theta_{mi} = \frac{t_i - t_m}{q_i'' D_h/k} = -\frac{\phi_m}{2(1 - r^*)} \tag{37}$$

$$\theta_{oi} - \theta_{mi} = \frac{t_o - t_m}{q_i'' D_h/k} = \frac{\phi_o - \phi_m}{2(1 - r^*)} \tag{38}$$

$$\theta_m = \frac{t_m - t_e}{q_i'' r_o/k} = \frac{4r^*\bar{x}}{1 + r^*} \tag{39}$$

The Nusselt number defined by $Nu_{ii} = h_{ii} D_h/k$, where $h_{ii} = q_i''/(t_i - t_m)$ may be written in terms of the fundamental solution variables as

$$Nu_{ii} = \frac{1}{\theta_{ii} - \theta_{mi}} \tag{40}$$

The circular tube and parallel plates represent extremes of the annulus with $r^* = 0$ and $r^* = 1$, respectively (except for the zero velocity boundary condition at the center of the circular tube) and are included to give a solution for a complete range of radius ratio. The solutions for these geometries were not obtainable from the annulus solution and had to be worked out separately.

The developing temperature profile for the circular tube was found to be of the form

$$\phi = \frac{t - t_o}{q_o'' r_o/k} = A_t \operatorname{ber}(\eta_o \bar{r}) + B_t \operatorname{bei}(\eta_o \bar{r}) + E_t \tag{41}$$

Using the results of the hydrodynamic solution of Langhaar [7], the thermal entry length solution for the circular tube was found in a similar method to that for the annulus. Likewise the parallel plates developing temperature profile was found to be

$$\phi = \frac{t - t_o}{q_o'' y_o/k} = A_t \sin(\eta\bar{y}) \sinh(\eta\bar{y}) + B_t \cos(\eta\bar{y}) \sinh(\eta\bar{y}) + C_t \sin(\eta\bar{y}) \cosh(\eta\bar{y}) + D_t \cos(\eta\bar{y}) \cosh(\eta\bar{y}) + E_t \tag{42}$$

and the solution was found using Han's [8] hydrodynamic results. Note that the coefficients A_t, B_t, . . . are different for each case, but the same symbols were kept to show the similarities. The details of the circular tube and parallel plates solutions are given in [9].

To complete the constant heat flux problem for the annulus, it is necessary to have a solution for the outer wall heated and the inner wall insulated. Then, by superposition, this solution plus the previously obtained solution for the inner wall heated and the outer wall insulated will give a solution for constant but unequal heat flux on both walls. The circular tube solution for practical purposes is the solution for an annulus with the outer tube heated and an infinitely small insulated core tube. The parallel plates solution represents a solution for an annulus with outer and inner tube radii equal and the outer wall heated and the inner wall insulated (or vice versa). Thus the solutions for the circular tube and parallel plates may be considered extreme ($r^* = 0$ and $r^* = 1$) solutions of the annulus with the outer wall heated and the inner wall insulated.

It was found that there was a relatively small difference between the results of the solutions for the circular tube and the parallel plates. Both the solutions approach the flat plate solution near the entrance and both approach a constant and not greatly different dimensionless temperature far downstream. Rather than carry out a separate solution for the annulus with heated outer wall and insulated inner wall, an interpolation was made between the solutions for the circular tube and the parallel plates. The interpolation was made for a given radius ratio by having the dimensionless wall temperature be in the same proportion between the circular tube and parallel plates solution in the developing region as it is for the fully developed condition using the solution for fully developed velocity and temperature given in [2]. The dimensionless mean temperature is given by $\theta_{mo} = 4\bar{x}/(1 + r^*)$. It was in this way that a solution was found for the annulus with outer wall heated and inner wall insulated.

4. THEORETICAL HEAT-TRANSFER RESULTS

The temperature variables of the fundamental solution of the second kind for the annulus are tabulated in Table 2 as a function of $\bar{x}$, r^* and Pr. The values given in the table were obtained from the numerical results of the solution by

Table 2. Results of the heat-transfer analysis for the annulus

$r^* = 0.02$										$r^* = 0.05$				
Inner wall heated										Inner wall heated				
	$Pr = 10.00$			$Pr = 0.70$			$Pr = 0.01$					$Pr = 0.70$		
$\bar{x}$	Nu_{ii}	$\theta_{ii}-\theta_{mi}$	$\theta_{oi}-\theta_{mi}$	Nu_{ii}	$\theta_{ii}-\theta_{mi}$	$\theta_{oi}-\theta_{mi}$	Nu_{ii}	$\theta_{ii}-\theta_{mi}$	$\theta_{oi}-\theta_{mi}$	θ_{mi}	$\bar{x}$	Nu_i	$\theta_{ii}-\theta_{mi}$	$\theta_{oi}-\theta_{mi}$	θ_{mi}
0.00010	87.2	0.0115	-0.0_5784	94.3	0.0106	-0.0_5784	—		-0.0_5784	0.0_57843	0.00010	70.3	0.0142	-0.0_4191	0.0_41905
0.0010	54.2	0.0185	-0.0_4784	53.5	0.0187	-0.0_4784	—		-0.0_4784	0.0_47843	0.0010	34.0	0.0294	-0.0_3191	0.0_31905
0.0025	46.6	0.0215	-0.0_3196	45.4	0.0220	-0.0_3196	46.0	0.0217	-0.0_3196	0.0_31961	0.0025	27.2	0.0368	-0.0_3476	0.0_34762
0.0050	41.9	0.0239	-0.0_3392	41.0	0.0244	-0.0_3392	40.5	0.0247	-0.0_3392	0.0_33922	0.0050	23.7	0.0422	-0.0_3952	0.0_39524
0.010	38.1	0.0263	-0.0_3784	37.4	0.0267	-0.0_3784	36.3	0.0275	-0.0_3784	0.0_37843	0.010	21.2	0.0472	-0.00191	0.001905
0.025	34.6	0.0289	-0.00173	34.4	0.0291	-0.00173	32.4	0.0309	-0.00183	0.001961	0.025	19.1	0.0525	-0.00417	0.004762
0.050	33.1	0.0302	-0.00236	33.1	0.0302	-0.00236	32.1	0.0312	-0.00201	0.003922	0.050	18.1	0.0553	-0.00565	0.009524
0.10	32.7	0.0306	-0.00255	32.7	0.0306	-0.00255	32.2	0.0311	-0.00205	0.007843	0.10	17.8	0.0561	-0.00610	0.01905
0.25	32.7	0.0306	-0.00256	32.7	0.0306	-0.00256	32.3	0.0310	-0.00220	0.01961	0.25	17.8	0.0561	-0.00613	0.04761
∞	32.7	0.0306	-0.00256	32.7	0.0306	-0.00256	32.7	0.0306	-0.00256	∞	∞	17.8	0.0561	-0.00613	∞
Outer wall heated										Outer wall heated				
	$Pr = 10.00$			$Pr = 0.70$			$Pr = 0.10$					$Pr = 0.70$		
$\bar{x}$	Nu_{oo}	$\theta_{oo}-\theta_{mo}$	$\theta_{io}-\theta_{mo}$	Nu_{oo}	$\theta_{oo}-\theta_{mo}$	$\theta_{io}-\theta_{mo}$	Nu_{oo}	$\theta_{oo}-\theta_{mo}$	$\theta_{io}-\theta_{mo}$	θ_{mo}	$\bar{x}$	Nu_{oo}	$\theta_{oo}-\theta_{mo}$	$\theta_{io}-\theta_{mo}$	θ_{mo}
0.00010	39.6	0.0253	-0.0_3392	52.2	0.0185	-0.0_3392	—	—	-0.0_3392	0.0_3392	0.00010	52.3	0.0183	-0.0_3381	0.0_33810
0.0010	14.78	0.0676	-0.00392	18.1	0.0553	-0.00392	24.2	0.0413	-0.00392	0.003922	0.0010	18.1	0.0552	-0.00381	0.003810
0.0025	10.49	0.0954	-0.00980	12.27	0.0315	-0.00980	15.9	0.0628	-0.00980	0.009804	0.0025	12.30	0.0813	-0.00952	0.009524
0.0050	8.35	0.1197	-0.0191	9.30	0.1075	-0.0196	11.9	0.0341	-0.0196	0.01961	0.0050	9.33	0.1072	-0.0191	0.01905
0.010	6.74	0.1483	-0.0391	7.34	0.1363	-0.0392	8.99	0.1112	-0.0392	0.03922	0.010	7.37	0.1358	-0.0381	0.03810
0.025	5.44	0.1838	-0.0363	5.72	0.1748	-0.0363	6.63	0.1496	-0.0940	0.09804	0.025	5.76	0.1737	-0.0833	0.09524
0.050	4.89	0.205	-0.118	5.02	0.1992	-0.0118	5.97	0.1676	-0.125	0.1961	0.050	5.07	0.1973	-0.113	0.1905
0.10	4.75	0.211	-0.127	4.77	0.210	-0.127	5.66	0.1768	-0.128	0.3922	0.10	4.83	0.207	-0.122	0.3810
0.25	4.73	0.211	-0.128	4.73	0.211	-0.128	5.42	0.1845	-0.128	0.9804	0.25	4.79	0.209	-0.123	0.9524
∞	4.73	0.211	-0.128	4.73	0.211	-0.128	4.73	0.211	-0.128	∞	∞	4.79	0.209	-0.123	∞

Table 2 continued

$r^* = 0{\cdot}10$										$r^* = 0{\cdot}25$				
Inner wall heated										Inner wall heated				
	$Pr = 10{\cdot}00$			$Pr = 0{\cdot}70$			$Pr = 0{\cdot}01$					$Pr = 0{\cdot}70$		
$\bar{x}$	Nu_{ii}	$\theta_{ii}-\theta_{mi}$	$\theta_{oi}-\theta_{mi}$	Nu_{ii}	$\theta_{ii}-\theta_{mi}$	$\theta_{oi}-\theta_{mi}$	Nu_{ii}	$\theta_{ii}-\theta_{mi}$	$\theta_{oi}-\theta_{mi}$	θ_{mi}	$\bar{x}$	Nu_{ii}	$\theta_{ii}-\theta_{mi}$	$\theta_{oi}-\theta_{mi}$	θ_{mi}
0·00010	51·2	0·0195	$-0{\cdot}0_4364$	61·2	0·0163	$-0{\cdot}0_4364$	—	—	$-0{\cdot}0_4364$	$0{\cdot}0_43636$	0·00010	55·4	0·0181	$-0{\cdot}0_4800$	$0{\cdot}0_48000$
0·0010	25·3	0·0395	$-0{\cdot}0_3364$	26·3	0·0330	$-0{\cdot}0_3364$	—	—	$-0{\cdot}0_3364$	$0{\cdot}0_33636$	0·0010	21·2	0·0472	$-0{\cdot}0_3800$	$0{\cdot}0_38000$
0·0025	20·1	0·0498	$-0{\cdot}0_3909$	20·1	0·0498	$-0{\cdot}0_3909$	21·7	0·0461	$-0{\cdot}0_3909$	$0{\cdot}0_39091$	0·0025	15·20	0·0658	−0·00200	0·002000
0·0050	17·1	0·0585	−0·00182	16·92	0·0591	−0·00182	17·8	0·0562	−0·00182	0·001818	0·0050	12·20	0·0820	−0·00400	0·004000
0·010	14·9	0·0671	0·00363	14·72	0·0697	−0·00364	14·8	0·0676	−0·00364	0·003636	0·010	10·28	0·0973	−0·00800	0·008000
0·025	12·9	0·0775	−0·00792	12·90	0·0775	−0·00792	12·4	0·0806	−0·00780	0·009091	0·025	8·57	0·1167	−0·0173	0·02000
0·050	12·13	0·08245	−0·0107	12·13	0·0824	−0·0107	11·8	0·0847	−0·00955	0·01818	0·050	7·94	0·1259	−0·0235	0·04000
0·10	11·92	0·08390	−0·0116	11·92	0·0839	−0·0116	11·71	0·0854	−0·0102	0·03636	0·10	7·77	0·1287	−0·0254	0·08000
0·25	11·91	0·08399	−0·0116	11·91	0·0840	−0·0116	11·76	0·0850	−0·0106	0·09091	0·25	7·75	0·1290	−0·0255	0·2000
∞	11·91	0·08399	−0·0116	11·91	0·0840	−0·0116	11·91	0·0840	−0·0116	∞	∞	7·75	0·1290	−0·0255	∞
Outer wall heated										Outer wall heated				
	$Pr = 10{\cdot}00$			$Pr = 0{\cdot}70$			$Pr = 0{\cdot}01$					$Pr = 0{\cdot}70$		
$\bar{x}$	Nu_{oo}	$\theta_{oo}-\theta_{mo}$	$\theta_{io}-\theta_{mo}$	Nu_{oo}	$\theta_{oo}-\theta_{mo}$	$\theta_{io}-\theta_{mo}$	Nu_{oo}	$\theta_{oo}-\theta_{mo}$	$\theta_{io}-\theta_{mo}$	θ_{mo}	$\bar{x}$	Nu_{oo}	$\theta_{oo}-\theta_{mo}$	$\theta_{io}-\theta_{mo}$	θ_{mo}
0·00010	39·7	0·0252	$-0{\cdot}0_3364$	52·3	0·0182	$-0{\cdot}0_3364$	—	—	$-0{\cdot}0_3364$	$0{\cdot}0_33636$	0·00010	52·4	0·0181	$-0{\cdot}0_3320$	$0{\cdot}0_33200$
0·0010	14·90	0·0671	−0·00364	18·1	0·0551	−0·00364	24·2	0·0413	−0·00364	0·003636	0·0010	18·2	0·0550	−0·00320	0·003200
0·0025	10·64	0·0940	−0·00909	12·32	0·0812	−0·00909	15·9	0·0629	−0·00909	0·009091	0·0025	12·36	0·0809	−0·00800	0·008000
0·0050	8·48	0·1179	−0·0182	9·35	0·1069	−0·0182	11·9	0·0843	−0·0182	0·01818	0·0050	9·38	0·1066	−0·0160	0·01600
0·010	6·86	0·1458	−0·0363	7·39	0·1353	−0·0364	8·96	0·1116	−0·0364	0·03636	0·010	7·43	0·1347	−0·0320	0·03200
0·025	5·54	0·1805	−0·0792	5·78	0·1729	−0·0792	6·65	0·1503	−0·0870	0·09091	0·025	5·83	0·1716	−0·0694	0·08000
0·050	4·98	0·200	−0·107	5·10	0·1960	−0·107	5·94	0·1634	−0·113	0·1818	0·050	5·16	0·1938	−0·0940	0·1600
0·10	4·85	0·206	−0·116	4·87	0·206	−0·116	5·64	0·1744	−0·116	0·3636	0·10	4·93	0·203	−0·102	0·3200
0·25	4·83	0·207	−0·116	4·83	0·207	−0·116	5·43	0·1843	−0·116	0·9091	0·25	4·91	0·204	−0·102	0·8000
∞	4·83	0·207	−0·116	4·83	0·207	−0·116	4·83	0·2069	−0·116	∞	∞	4·91	0·204	−0·102	∞

Table 2 continued

$r^* = 0.50$

Inner wall heated

	$Pr = 10.00$			$Pr = 0.70$			$Pr = 0.01$			
$\bar{x}$	Nu_{ii}	$\theta_{ii}-\theta_{mi}$	$\theta_{oi}-\theta_{mi}$	Nu_{ii}	$\theta_{ii}-\theta_{mi}$	$\theta_{oi}-\theta_{mi}$	Nu_{ii}	$\theta_{ii}-\theta_{mi}$	$\theta_{oi}-\theta_{mi}$	θ_{mi}
0.00010	—	—	-0.0_3133	53.5	0.0186	-0.0_3133	—	—	-0.0_3133	0.0_31333
0.0010	16.86	0.0592	−0.00133	19.22	0.05203	−0.00133	—	—	−0.00133	0.001333
0.0025	12.60	0.0794	−0.00333	13.46	0.07429	−0.00333	—	—	−0.00333	0.003333
0.0050	10.20	0.0980	−0.00667	10.47	0.09551	−0.00667	—	—	−0.00667	0.006667
0.010	8.43	0.1186	−0.0133	8.52	0.1174	−0.0133	9.43	0.1060	−0.0133	0.01333
0.025	6.93	0.1443	−0.0289	6.98	0.1433	−0.0289	7.05	0.1418	−0.0289	0.03333
0.050	6.35	0.1574	−0.0392	6.35	0.1575	−0.0392	6.40	0.1563	−0.0392	0.06667
0.10	6.19	0.1615	−0.0425	6.19	0.1616	−0.0425	6.22	0.1608	−0.0425	0.1333
0.25	6.18	0.1618	−0.0428	6.18	0.1618	−0.0428	6.18	0.1618	−0.0428	0.3333
∞	6.18	0.1618	−0.0428	6.18	0.1618	−0.0428	6.18	0.1618	−0.0428	∞

Outer wall heated

	$Pr = 10.00$			$Pr = 0.70$			$Pr = 0.01$			
$\bar{x}$	Nu_{oo}	$\theta_{oo}-\theta_{mo}$	$\theta_{io}-\theta_{mo}$	Nu_{oo}	$\theta_{oo}-\theta_{mo}$	$\theta_{io}-\theta_{mo}$	Nu_{oo}	$\theta_{oo}-\theta_{mo}$	$\theta_{io}-\theta_{mo}$	θ_{mo}
0.0010	40.0	0.0250	-0.0_3267	52.5	0.0178	-0.0_3267	—	—	-0.0_3267	0.0_32667
0.0010	15.14	0.0660	−0.00267	18.3	0.0547	−0.00267	24.2	0.0413	−0.00267	0.002667
0.0025	10.94	0.0914	−0.00667	12.42	0.0805	−0.00667	15.9	0.0630	−0.00667	0.006667
0.0050	8.75	0.1143	−0.0133	9.45	0.1058	−0.0133	11.8	0.0847	−0.0133	0.01333
0.010	7.09	0.1410	−0.0266	7.50	0.1334	−0.0267	8.90	0.1123	−0.0267	0.02667
0.025	5.74	0.1741	−0.0568	5.91	0.1692	−0.0568	6.59	0.1518	−0.0630	0.06667
0.050	5.20	0.1925	−0.0784	5.27	0.1899	−0.0784	5.88	0.1702	−0.0820	0.1333
0.10	5.05	0.1979	−0.0851	5.06	0.1975	−0.0851	5.60	0.1786	−0.0855	0.2667
0.25	5.04	0.1985	−0.0855	5.04	0.1985	−0.0855	5.44	0.1837	−0.0855	0.6667
∞	5.04	0.1985	−0.0855	5.04	0.1985	−0.0855	5.04	0.1986	−0.0855	∞

careful interpolation at convenient values of $\bar{x}$ to aid in superposition. The inner tube heated results were obtained directly from the analysis while the outer tube heated results were obtained from the circular tube and parallel plates solutions as described previously. The results for the circular tube and parallel plates are tabulated in Table 3.

The results are presented in terms of the nomenclature for the fundamental solution of the second kind introduced in [1]. The format is consistent with that of the results presented in [2] for fully developed velocity throughout. This latter solution may be interpreted as a developing velocity problem with Prandtl number very large or approaching infinity. Thus the results in [2] can be used conveniently to extend the present solution to larger values of Prandtl number.

In Fig. 5 are plotted the results of Nu as a function of $\bar{x}$ for $Pr = 0.7$ with r^* as a parameter. Shown as a dotted line to the left is the solution for a flat plate applied to the annulus variables and with free stream velocity taken to be the velocity outside the boundary layers. The dotted lines to the right represent fully developed solutions. Both the core tube and outer tube heated solutions are represented. The curves above $r^* = 1$ represent the core tube heated and those below represent the outer tube heated. In Fig. 6 are shown the results of Nusselt number for inner wall heated as a function of

Table 3. Results of the heat-transfer analysis for the parallel plates and circular tube

Parallel plates ($r^* = 1{\cdot}0$)

	$Pr = 10{\cdot}00$			$Pr = 0{\cdot}70$			$Pr = 0{\cdot}01$			
$\bar{x}$	Nu_{oo}	$\theta_{oo}-\theta_{mo}$	$\theta_{io}-\theta_{mo}$	Nu_{oo}	$\theta_{oo}-\theta_{mo}$	$\theta_{io}-\theta_{mo}$	Nu_{oo}	$\theta_{oo}-\theta_{mo}$	$\theta_{io}-\theta_{mo}$	θ_{mo}
0·00010	40·4	0·0248	$-0{\cdot}0_3200$	52·8	0·0172	$-0{\cdot}0_3200$	—	—	$-0{\cdot}0_3200$	$0{\cdot}0_32000$
0·0010	15·56	0·0643	−0·00200	18·50	0·0541	−0·00200	24·2	0·0413	−0·00200	0·002000
0·0025	11·46	0·0873	−0·00500	12·60	0·0794	−0·00500	15·8	0·0633	−0·00500	0·005000
0·0050	9·20	0·1087	−0·0100	9·62	0·1040	−0·0100	11·7	0·0855	−0·0100	0·01000
0·010	7·49	0·1335	−0·0199	7·68	0·1302	−0·0200	8·80	0·1136	−0·0200	0·02000
0·025	6·09	0·1643	−0·0433	6·13	0·1631	−0·0433	6·48	0·1543	−0·0480	0·05000
0·050	5·55	0·1803	−0·0589	5·55	0·1802	−0·0589	5·77	0·1733	−0·0655	0·1000
0·10	5·40	0·1854	−0·0639	5·40	0·1854	−0·0639	5·53	0·1808	−0·0680	0·2000
0·25	5·39	0·1857	−0·0643	5·39	0·1857	−0·0643	5·47	0·1828	−0·0660	0·5000
∞	5·39	0·1857	−0·0643	5·39	0·1857	−0·0643	5·39	0·1857	−0·0643	∞

Circular tube ($r^* = 0$)

	$Pr = 10{\cdot}00$			$Pr = 0{\cdot}70$			$Pr = 0{\cdot}01$			
$\bar{x}$	Nu_{oo}	$\theta_{oo}-\theta_{mo}$	$\theta_{co}-\theta_{mo}$	Nu_{oo}	$\theta_{oo}-\theta_{mo}$	$\theta_{co}-\theta_{mo}$	Nu_{oo}	$\theta_{oo}-\theta_{mo}$	$\theta_{co}-\theta_{mo}$	θ_{mo}
0·00010	39·1	0·0256	$-0{\cdot}0_3400$	51·9	0·0193	$-0{\cdot}0_3400$	—	—	$-0{\cdot}0_3400$	$0{\cdot}0_34000$
0·0010	14·34	0·0697	−0·00400	17·84	0·0561	−0·00400	24·2	0·0413	−0·00400	0·004000
0·0025	9·93	0·1007	−0·0100	12·08	0·0828	−0·0100	16·0	0·0625	−0·0100	0·01000
0·0050	7·87	0·1271	−0·0200	9·12	0·1096	−0·0200	12·0	0·0833	−0·0200	0·02000
0·010	6·32	0·1582	−0·0400	7·14	0·1401	−0·0400	9·10	0·1099	−0·0400	0·04000
0·025	5·07	0·1972	−0·0882	5·49	0·1821	−0·0882	6·80	0·1471	−0·0960	0·1000
0·050	4·51	0·222	−0·135	4·72	0·212	−0·135	6·08	0·1645	−0·132	0·2000
0·10	4·38	0·228	−0·143	4·41	0·227	−0·143	5·73	0·1745	−0·136	0·4000
0·25	4·36	0·229	−0·146	4·36	0·229	−0·146	5·39	0·1855	−0·136	1·000
∞	4·36	0·229	−0·146	4·36	0·229	−0·146	4·36	0·229	−0·146	∞

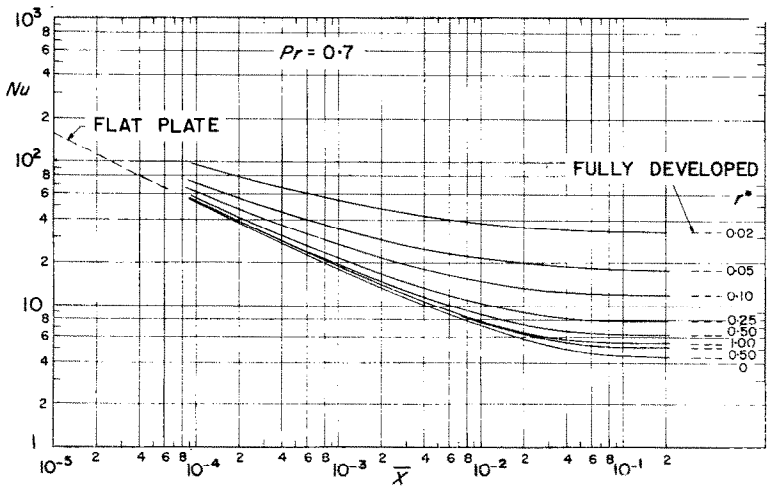

FIG. 5. Results of the heat-transfer analysis for Prandtl number = 0·7 and various radius ratios.

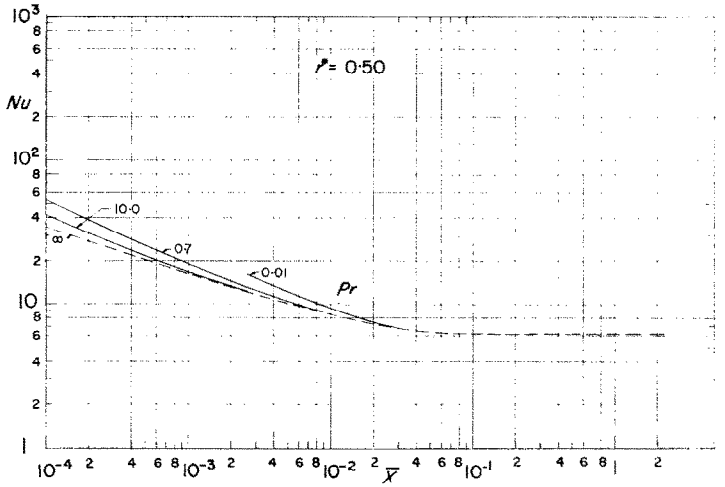

FIG. 6. Results of the heat-transfer analysis for the inner wall heated with radius ratio = 0·50 and various Prandtl numbers.

$\bar{x}$ for $r^* = 0{\cdot}5$ and Prandtl number as a parameter. The dotted line is Lundberg's [2] fully developed flow solution which represents the limiting case as $Pr \to \infty$.

The heat-transfer results presented thus far give the solution only for one wall heated and the other wall insulated. By superposition [1] these results may be extended to the case of each wall heated with constant and unequal heat flux. If the heat flux on each wall is given to be

$$q_i'' = q_i/A_i, \qquad q_o'' = q_o/A_o$$

then the mixed-mean fluid temperature and inner and outer wall temperatures may be calculated from,

$$\left.\begin{aligned} t_m &= \frac{D_h}{k}\,[q_i''\theta_{mi} + q_o''\theta_{mo}] + t_e \\ t_i &= \frac{D_h}{k}\,[q_i''\theta_{ii} + q_o''\theta_{io}] + t_e \\ t_o &= \frac{D_h}{k}\,[q_i''\theta_{oi} + q_o''\theta_{oo}] + t_e \end{aligned}\right\} \quad (43)$$

5. EXPERIMENTAL HEAT-TRANSFER RESULTS

Wall temperature measurements were made on the annulus apparatus described in [1]. The apparatus consisted of 1 in and 2 in Inconel outer tubes, and a 0·058 in stainless steel core tube and $\frac{3}{8}$ in and $\frac{1}{2}$ in Inconel core tubes, giving a total of six different radius ratio annuli. Air from a plenum chamber passed through two screens and a smooth nozzle attached to the outer tube giving an initial velocity which was uniform to ± 2 per cent for the 2 in tube and $\pm 0{\cdot}5$ per cent for the 1 in tube. Either the core tube or the outer tube was heated electrically from the entrance to produce a constant heat flux to the air. The unheated tube was nickel-plated to reduce radiation exchange between the two tubes. The outer tube was insulated to reduce heat loss to the surroundings.

The temperature, heat flux and fluid flow measurements were reduced to Nu_{ii} or Nu_{oo} as a function of $\bar{x}$. In the data reduction a correction was made for radiation loss from the heated wall and the fact that the unheated wall was actually heated slightly by radiation from the opposite wall. The heat-transfer results are shown plotted in Figs. 7 and 8 for the inner wall heated. The data for each radius ratio represent four or five runs made with a Reynolds number variation of about 1000 to 5500. The solid line represents the analysis.

The probable uncertainty in the experimental results is about ± 9 per cent for the two larger core tubes in the 2 in outer tube and about ± 6 per cent for the other tube combinations. The greatest factor in the uncertainty comes from predicting the radiation exchange between

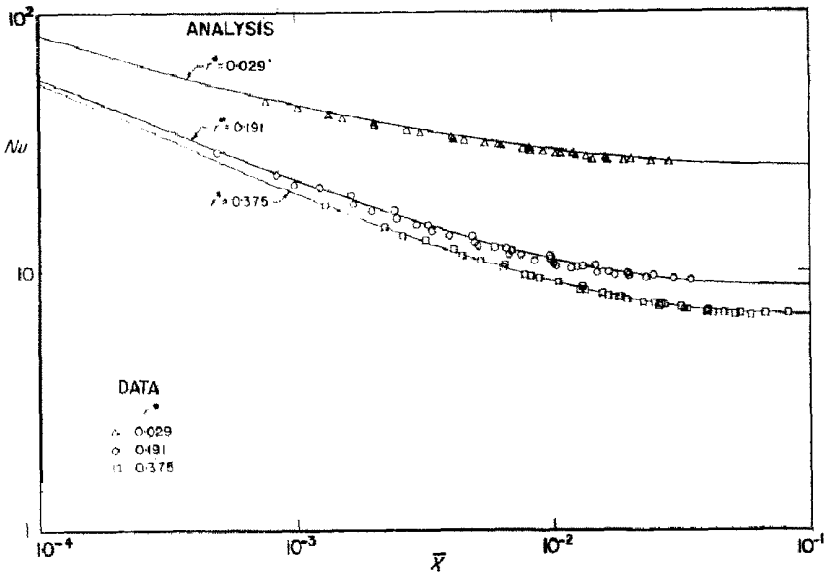

FIG. 7. Comparison of the heat-transfer analysis with the experimental results for the inner wall heated and radius ratio = 0·029, 0·191, 0·375.

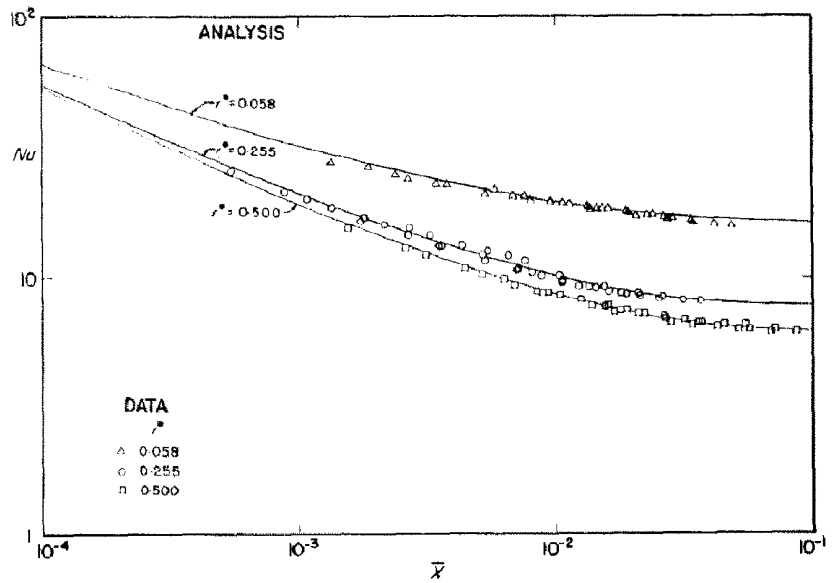

FIG. 8. Comparison of the heat-transfer analysis with the experimental results for the inner wall heated and radius ratio = 0·058, 0·255, 0·500.

the two tubes. The emissivity was assumed to be 0·2 for the Inconel and stainless tubes and 0·1 for the nickel-plated Inconel tube.† As it turned out the radiation correction was greatest for $r^* = 0{\cdot}191$ and 0·255 and this is the reason for the greatest uncertainty for these two annuli. It is noted that the data scatter is also greatest for these two annuli.

The experimental results generally agree with the analysis well within the experimental uncertainty. The excellent agreement between the experimental data and the analysis show that the results in Table 2 represent an accurate solution for $Pr = 0{\cdot}7$ and provide confidence in the solutions for other Prandtl numbers.

6. CONCLUDING REMARKS

The results of the heat-transfer analysis provide a solution to the problem of heat transfer in an annulus with constant heat flux and simultaneously developing velocity and temperature distributions. Even though the boundary conditions are for one wall heated and one wall insulated, it is possible by superposition to extend this to the case of constant but unequal heat flux on each wall. The solution as it stands cannot handle axially varying wall heat flux, but using the same technique it could be extended to do this.

The solution while it applies only to laminar flow, can be very useful for some cases of turbulent flow. Where heating begins from the entrance of an annulus, the presence of a short length of laminar flow can cause initially higher wall temperatures than predicted from turbulent flow for constant wall heat flux. This was observed experimentally.

In designing an annulus for turbulent flow, special care must be taken if heating is to begin at the entrance to avoid excessively high wall temperatures in the laminar region.

† A value of 0·35 was used for Inconel in [9]. A further search of the available literature has shown 0·20 is a more realistic value.

REFERENCES

1. W. C. Reynolds, R. E. Lundberg and P. A. McCuen, Heat transfer in annular passages. General formulation of the problem for arbitrarily prescribed wall temperatures or heat fluxes, *Int. J. Heat Mass Transfer* **6**, 483–493 (1963).
2. R. E. Lundberg, P. A. McCuen and W. C. Reynolds, Heat transfer in annular passages. Hydrodynamically developed laminar flow with arbitrarily prescribed wall temperatures or heat fluxes, *Int. J. Heat Mass Transfer* **6**, 495–529 (1963).
3. W. M. Kays and E. Y. Leung, Heat transfer in annular passages. Hydrodynamically developed turbulent flow with arbitrarily prescribed heat flux, *Int. J. Heat Mass Transfer* **6**, 537–557 (1963).
4. K. Murakawa, Heat transfer in entry length of double pipes, *Int. J. Heat Mass Transfer* **2**, 240–251 (1961).
5. L. Schiller, Die entwicklung der laminaren geschwindigkeitverteilung und ihre bedeutung für zähigkeitsmessungen, *Z. Angew. Math. Mech.* **2**, 96 (1922).
6. E. M. Sparrow, Analysis of laminar forced-convection heat transfer in entrance region of flat rectangular ducts, *NACA TN* 3331 (1955).
7. H. L. Langhaar, Steady flow in the transition length of a straight tube, *J. Appl. Mech.* **9**, A55–A58 (1942).
8. L. S. Han, Hydrodynamic entrance lengths for incompressible laminar flow in rectangular ducts, *J. Appl. Mech.* **27** 403–410 (1960).
9. H. S. Heaton, W. C. Reynolds and W. M. Kays, Heat transfer with laminar flow in concentric annuli with constant heat flux and simultaneously developing velocity and temperature distributions, Ph.D. Dissertation, Stanford University (1962). See also Department of Mechanical Engineering Report *AHT*-5, Stanford University (1962).
10. W. M. Kays, Numerical solutions for laminar-flow heat transfer in circular tubes, *Trans. Amer. Soc. Mech. Engrs.* **77**, 1265–1274 (1955).
11. P. Goldberg, M. S. Thesis, Mechanical Engineering Department, M.I.T. (1958). See also W. M. Rohsenow and H. Y. Choi, *Heat, Mass and Momentum Transfer*, p. 149. Prentice-Hall, New Jersey (1961).
12. M. Sibahayasi and E. Sugino, On the temperature distribution at the laminar inlet in a circular pipe, *Proc. 6th Japan Nat. Congress for Appl. Mech.* III-5, pp. 389–392 (1956).
13. R. Siegel and E. M. Sparrow, Simultaneous development of velocity and temperature distributions in a flat duct with uniform wall heating, *J. Amer. Inst. Chem. Engrs* **5**, 73–75 (1959).
14. L. S. Han, Simultaneous developments of temperature and velocity profiles in flat ducts, International Heat Transfer Conference, paper 70, pp. 591–597 (1961).

Résumé—On analyse le problème du transport de chaleur en écoulement laminaire dans un conduit annulaire avec des distributions de vitesse et de température se développant en même temps et un flux de chaleur pariétal constant. On obtient d'abord une solution du problème hydrodynamique et ensuite du problème combiné hydrodynamique et thermique par une méthode intégrale. Les résultats

sont mis sous la forme de tableaux pour plusieurs rapports du rayon du tube intérieur à celui du tube extérieur et plusieurs nombres de Prandtl. Les mesures expérimentales faites pour le nombre de Prandtl 0,7 montraient un accord excellent avec l'analyse théorique. Cet article est le quatrième d'une série terminant une étude de quatre années sur le transport de chaleur dans les conduits annulaires.

Zusammenfassung—Das Problem des Wärmeüberganges bei Laminarströmung in einem Ringraum, in dem sich bei konstanter Wärmestromdichte gleichzeitig ein Geschwindigkeits- und ein Temperaturfeld aufbaut, wird analytisch untersucht. Nach einer Integralmethode erhält man erst eine Lösung für das hydrodynamische Problem und dann für die Kombination des hydrodynamischen mit dem thermischen Problem. Die Ergebnisse für verschiedene Verhältnisse von Innen- und Aussendurchmesser und verschiedene Prandtl-Zahlen sind tabelliert. Experimentelle Messungen für eine Prandtl-Zahl von 0,7 ergaben sehr gute Übereinstimmung mit der Analyse. Diese Arbeit ist die vierte einer Reihe über eine vierjährige Untersuchung des Wärmeüberganges in Ringräumen.

Аннотация—Анализируется задача теплообмена при ламинарном течении в кольцевом канале при одновременном развитии полей скорости и температуры, и постоянном тепловом потоке на стенке. Путем интегрального метода получено решение для гидродинамической задачи, а также для совместной гидродинамической и тепловой задач. Результаты протабулированы для нескольких отношений внутренних радиусов к внешним для различных чисел Прандтля. Экспериментальные измерения, проведенные для $Pr = 0{,}7$, показали хорошую согласованность с теоретическими данными. Эта статья является четвертой в серии статей и подытоживает четырехлетнее изучение теплообмена в кольцевых каналах.